Dalton Transactions

PAPER

View Article Online
View Journal | View Issue

Cite this: *Dalton Trans.*, 2016, **45**, 8790

Dinuclear dysprosium SMMs bridged by a neutral bipyrimidine ligand: two crystal systems that depend on different lattice solvents lead to a distinct slow relaxation behaviour†

Wen-Bin Sun,[a,b] Bing Yan,[a] Li-Hui Jia,[c] Bing-Wu Wang,*[a] Qian Yang,[a] Xin Cheng,[a] Hong-Feng Li,[b] Peng Chen,[b] Zhe-Ming Wang[a] and Song Gao*[a]

Received 20th March 2016,
Accepted 19th April 2016

DOI: 10.1039/c6dt01082b

www.rsc.org/dalton

Two dinuclear dysprosium complexes with the Dy(III) ions bridged by the neutral bipyrimidine (BPYM) ligand were synthesized and magnetically characterized. They crystallized in a monoclinic and triclinic crystal system, respectively, with almost the same structural core, only differing in the lattice solvent molecules. Alternating current (ac) susceptibility measurements revealed that they exhibit significant slow relaxation of magnetization until 25 K in the absence of a dc field. The single and double relaxation processes were assigned to one and two types of Dy(III) environments in the two dimmers, respectively, with barriers of 266 and 345 K under zero field conditions. The magnetic hysteresis loops of 1 and 2 were both observed up to 2.5 K.

Since the first double decker phthalocyanine (Pc) complexes, $[Bu_4N][LnPc_2]$ with Ln = Tb and Dy as the mononuclear single-molecule magnet (SMM) were reported,[1] the investigations on these lanthanide-based SMMs keep attracting the increasing attention due to their potential technological applications in the field of quantum computing, spintronic devices and high-density information storage.[2–7] The intrinsic strong spin–orbit coupling and large magnetic moment render the lanthanide(III) ions excellent candidates for building SMMs, especially for a system with a single spin center. Such molecular systems are commonly referred to as mononuclear SMMs or single-ion magnets (SIMs). The high spin reversal barriers (U_{eff}) and blocking temperature (T_B) are accessible in these mononuclear lanthanide SMMs due to the significant single-ion magnetic anisotropy delivered by an appropriate configuration of the 4f electrons. To date, both the highest U_{eff} and T_B are recorded by the 4f-based SMMs.[8–10] Although the record of U_{eff} has been broken continually, as large as 652 cm^{-1},[8] the highest T_B is only 14 K for a dinuclear Tb_2 SMM, and recently a 20 K T_B was reached by a mononuclear Dy-based SMM.[10] An efficient way to enhance the single-ion magnetic anisotropy is by tuning the symmetry and strength of the local ligand field to improve the relaxation performance of SIMs. However, the quantum tunnelling of magnetization (QTM) often shortcuts the thermal relaxation barrier and eliminates the remnant magnetization in a typical hysteresis measurement. Some strategies that could reduce or suppress the QTM are for example, applying an external direct current (dc) field or diluting samples by similar diamagnetic lanthanide congeners to reduce the intermolecule dipolar–dipolar interactions. In addition, suitable magnetic exchange interactions have been shown to hinder and enhance magnetic relaxation in different examples and a 14 K T_B was observed in a dinuclear Tb_2N_2 system with strong magnetic exchange coupling.[10]

Despite the many efforts that have been devoted to lanthanide-centered magnetic systems, and much remarkable progress has been obtained, many open questions remain on the magnetic relaxation properties of these molecules, in particular, the relaxation mechanism in these systems is often very complicated. The different environments surrounding the spin center usually lead to distinct dynamic magnetic relaxation processes that are usually attributed to an Orbach mechanism. However, the different pathways for magnetic relaxation involving QTM, direct and Raman processes have also been detected in recent studies.[11] For the limited measured temperature range and dynamic magnetic field, clarification of

[a]*Beijing National Laboratory of Molecular Science State Key Laboratory of Rare Earth Materials Chemistry and Applications, College of Chemistry and Molecular Engineering, Peking University, Beijing 100871, China. E-mail: wangbw@pku.edu.cn, gaosong@pku.edu.cn*

[b]*Department Key Laboratory of Functional Inorganic Material Chemistry Ministry of Education, Heilongjiang University, Harbin 150080, China*

[c]*School of Chemistry and Environmental Engineering, Wuhan Institute of Technology, Wuhan 430073, P. R. China*

† Electronic supplementary information (ESI) available: Synthesis details, crystallographic data, additional magnetic data, additional figures. CCDC 962684 and 962685 for **1** and **2**. For ESI and crystallographic data in CIF or other electronic format see DOI: 10.1039/c6dt01082b

the dynamics derived from different relaxation sources and pathways for magnetic relaxation remains a challenge. Relaxation in mononuclear SMMs is often induced by the spin–lattice interaction, whereas the static electric field, which is named the ligand field for a molecule, does not easily affect the shielded 4f electrons from the outer filled 5s and 5p orbitals. Recent developments in the lanthanide-based SMMs shows that even subtle changes of the ligand field can drastically influence the overall magnetic properties of SMMs. It provides an opportunity to control the local magnetic anisotropy by tuning the ligand field, a relatively high axial symmetry is normally favourable. It could be predicted that combining axial symmetry with a suitable magnetic exchange interaction, even a very weak interaction, may generate a high performance SMM system.

Taking account of our recent work on mono-dysprosium β-diketonate SMMs that have a simple structure but suffered the QTM effect,[12] we tried to link the β-diketonated SIMs moiety through a bridging bipyrimidine (BPYM) ligand, which is a useful double bidentate ligand involving N atoms, to build binuclear lanthanide compounds.[13] BPYM possesses a rigid coplanar and delocalized aromatic conjugated electronic structure and shows the ability to transmit magnetic interactions for orbital overlapping of spin centers. The radical BPYM has been used to build a dinuclear Dy_2 SMM system in which the efficient antiferromagnetic interaction benefits their SMMs behaviour.[14] Although only very weak magnetic coupling could be transmitted between f electrons by the neutral bridge ligand,[9,10,15] it seems large enough to influence the magnetic dynamics. In line with this strategy, dinuclear complexes possessing two mononuclear β-diketonate Dy(III) moieties bridged by the neutral BPYM were synthesized (Scheme 1).

The pure compounds were crystallized from chloroform–methanol and dried under vacuum for hours. To get the pure crystallized product, they were recrystallized from the pure solution of chloroform ($CHCl_3$) and acetonitrile (MeCN) respectively. Thus, crystalline complexes of $[(DBM)_6Dy_2BPYM]\cdot 2CHCl_3$ (**1**) and $[(DBM)_6Dy_2BPYM]\cdot MeCN$ (**2**) were obtained. Interestingly, they crystallized in monoclinic and triclinic crystal systems, respectively. Complex **1** and **2** have similar local coordination cores but differ in the lattice solvents. The representative structure of **1** is depicted in Fig. 1. It crystallizes in a monoclinic $P21/c$ space group in which six oxygen atoms from three DBM ligands coordinate the Dy1 and Dy2 centers, respectively. The bridging ligand BPYM provides two bidentated nitrogen atoms to complete the eight-coordinated geometry of each Dy(III) ion. The shortest intermolecular Dy···Dy distances are 11.168 Å and 8.856 Å in **1** and **2** respectively, albeit the weak π–π interaction (Fig. S1†) exists and the Dy(III) centers can be considered to be isolated from their adjacent molecules from a magnetic point of view.

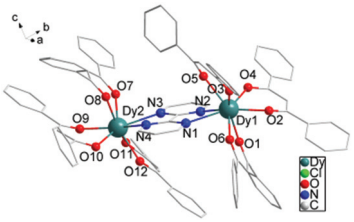

Fig. 1 Structure of complex **1**, the H atoms and $CHCl_3$ molecule are omitted for clarity.

The coordination environments of Dy1 and Dy2 are different in **1**. Using the continuous-shape-measures (CShMs) method,[16] it gives the smallest deviation parameter of 0.846 for Dy1 compared to the ideal D_{2d} triangular dodecahedron. For Dy2, the smallest deviation parameter compared to the ideal D_{4d} square antiprism geometry is 0.947 (Table S2†). As for the structure of **2** depicted in Fig. S1,† it crystallizes in a triclinic $P\bar{1}$ space group. The centrosymmetric geometry of the molecule makes the coordination environment of the two Dy(III) ions be identical with a coordination symmetry close to the ideal D_{2d} (Table S2†).

Variable temperature dc magnetic data (χT *vs.* T plots) for **1** and **2** (Fig. S2 and 3†) show that the room temperature χT values for **1** and **2** are 28.1 cm^3 K mol^{-1} and 28.9 cm^3 K mol^{-1}, respectively, which are in good agreement with the theoretical values of 28.34 cm^3 K mol^{-1} for two non-interacting Dy(III) ions ($S = 5/2$, $L = 5$, $^6H_{15/2}$, $g = 4/3$). The χT values decrease slowly with lowering of the temperature before 6 K, then drop rapidly to 20.2 cm^3 K mol^{-1} (**1**) and 23.1 cm^3 K mol^{-1} (**2**) at 2K. Magnetization plots (M *vs.* H and M *vs.* H/T) for **1** and **2** (Fig. S4 and S5† respectively) in the temperature range 2–8 K at high fields (up to 5 T) show non-saturation as well as non-superposition on a single curve, indicating the presence of magneto-anisotropy and/or low-lying excited states.

Alternating current (ac) susceptibility measurements on **1** and **2** displayed significant ac peaks under zero field at a relative high temperature range between 5.5 K and 25 K, which is indicative of the prevalent SMM behaviour in these two systems (Fig. 2 and S7–13†).

For **1**, the temperature dependent out-of-phase ac susceptibilities display two distinct peaks between 5.5 K (100 Hz) and 25 K (10 000 Hz), which indicate two relaxation processes dominate this system. The low temperature one (R_{LT}) and high temperature one (R_{HT}) could be ascribed to the two different Dy(III) ions centers (D_{2d} symmetry for Dy1 and D_{4d} symmetry for Dy2) in **1**. Only one frequency dependent peak was detected for **2** between 12.5 K (100 Hz) and 25 K (10 000 Hz), which is indicative of the occurrence of one relaxation process deriving from the single Dy(III) center in **2**. The single and dual relax-

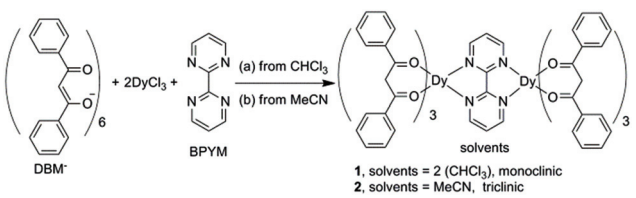

Scheme 1 Synthesis of complexes **1** and **2**, recrystallized from $CHCl_3$ and MeCN respectively, resulting in different crystal systems.

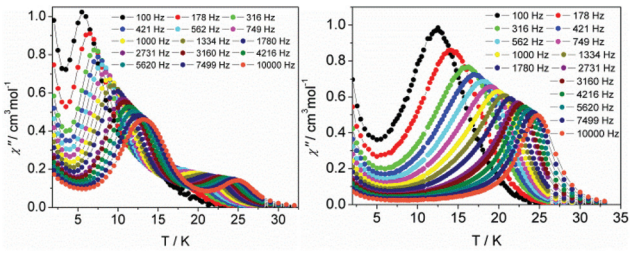

Fig. 2 Temperature dependence of the out-of phase χ'' ac susceptibility signals for **1** (left) and **2** (right) under zero applied field.

ation processes can be clearly identified in the Cole–Cole plots for **1** and **2** under zero field (Fig. S14†) conditions. The increasing χ'' below 5 K indicates the intervention of QTM. The temperature and frequency dependent ac susceptibility were measured under an applied 1500 Oe field (Fig. S10–S13†). The diminishing of the upward χ'' under low temperatures reveal that the QTM was suppressed efficiently. Clear double and single relaxation processes are still detected in **1** and **2** under an applied 1500 Oe field, respectively.

In order to further probe the source of these slow magnetic relaxations, the samples were diluted by a diamagnetic matrix of Y(III) analogous with Dy : Y molar ratio 1 : 20, **1a** and **2a**. The similar temperature and frequency dependent ac susceptibility performance at the high temperature range between undiluted and diluted samples indicate that the slow magnetic relaxations come mainly from the single Dy(III) center (Fig. S15–S22†).

For an Orbach-type relaxation, the relaxation time and barrier will follow an Arrhenius law ($\tau = \tau_0 \exp(U_{eff}/kT)$, $\tau = 1/2\pi\nu$, at $\nu = \chi''_{max}$) in which a linear relationship between $\ln(\tau)$ and $1/T$ should be observed. In our case, however, their relationship displays curvilinear plots that are commonly proposed to be QTM for this phenomenon, especially in the low temperature region in the absence of a dc field. But for our case, after the combination of both applying an external dc field and performing the magnetic dilution (Fig. 3, Tables S3 and S4†), the deviation from the Arrhenius-type linearity was still apparent. It may be the presence of multiple relaxation processes besides the Orbach process, which was also observed in a few SIMs.[11d,17,18] In view of this, we fitted the magnetic

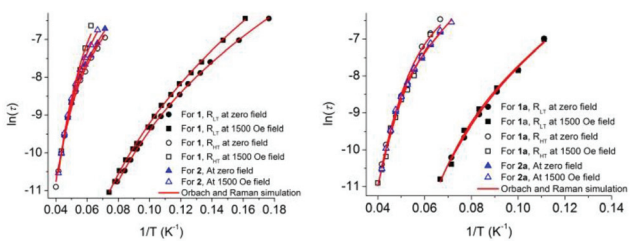

Fig. 3 Plots of $\ln(\tau)$ *vs.* T^{-1} for the undiluted (left, **1** and **2**) and diluted samples (right, **1a** and **2a**) under zero and 1500 Oe field, respectively. Red lines correspond to the fitted results combining Orbach and Raman relaxation processes.

data with the following equation considering the spin–lattice relaxation occurring through both Raman and Orbach processes:[19]

$$1/\tau = CT^n + \tau_0^{-1} \exp(-U_{eff}/kT) \quad (1)$$

The first and second terms correspond to the Raman and Orbach processes, respectively. In general, $n = 9$ for Kramers ions, but when both the acoustic and optical phonons are considered, depending on the structure of energy levels, n values between 1 and 6 are reasonable.[19,20]

The modified Arrhenius law fitting gives rise to energy barriers (Fig. 3) of $U_{eff}/k = 120$ K with $\tau_0 = 5.6 \times 10^{-9}$ s under zero field and $U_{eff}/k = 154$ K with $\tau_0 = 1.5 \times 10^{-10}$ s under 1500 Oe field for the R_{LT} of **1**. As a comparison, the energy barriers extracted from the high temperature regions of the Arrhenius plots U_{Orb}/k are 67 K and 87 K under zero and 1500 Oe external fields, respectively (Table S4†).

For the R_{HT} process of **1**, U_{eff}/k of 266 K with $\tau_0 = 6.4 \times 10^{-10}$ s, and $U_{Orb}/k = 201$ K under zero-field and U_{eff}/k of 287 K with $\tau_0 = 2.0 \times 10^{-10}$ s and $U_{Orb}/k = 215$ K under 1500 Oe field are obtained, respectively (Tables S3 and S4†). As for complex **2**, similar with **1**, the Orbach mixed Raman relaxation processes manipulate the system. The relative higher energy barriers $U_{eff}/k = 345$ K with $\tau_0 = 2.1 \times 10^{-11}$ s and $U_{eff}/k = 350$ K with $\tau_0 = 1.7 \times 10^{-11}$ s are obtained under zero and 1500 Oe dc field fitting by eqn (1), respectively, and U_{Orb}/k is 267 K and 279 K extracted from the thermally activated Orbach process (Tables S3 and S4). These energy barriers are significantly higher than the former reported Dy(III)-based SIMs built by three acetylacetone (acac) ligands and one 1,10-phenanthroline (phen) or its derivatives.[21,22] It is also noteworthy that, only from the symmetry point of view, the Dy(III) center in **2**, possessing nearly D_{2d} local symmetry, leads to a relative high higher energy barrier of 345 K under zero dc field; therefore, the two distinct R_{HT} and R_{LT} processes in **1** could be tentatively assigned to the Dy1 (D_{2d}) and Dy2 (D_{4d}) sources, respectively. To confirm the distinct relaxation behaviour for **1** and **2** are derived from their individually intrinsic molecule source, the dynamic magnetic properties of their diluted samples **1a** and **2a** were studied (Fig. S14–S21†). The diminishing χ'' signals in the plot of temperature and frequency dependent ac susceptibility indicates the QTM was suppressed efficiently. The larger separation between molecules reduced the dipolar–dipolar intermolecular coupling. The nearly identical temperature and frequency dependent behaviour of ac susceptibility between undiluted and diluted samples reveal that the magnetic relaxations in **1** and **2** are derived from their individually intrinsic molecule source.

Hysteresis is also an important characteristic of magnetic bi-stability for a magnet. The magnetizations (M) *versus* applied dc field for **1** and **2** were performed on polycrystalline samples with a sweep rate (about 100–300 Oe min^{-1}) used in a traditional SQUID XL-5 magnetometer, and a significant hysteresis could be detected under 2.5 K both for **1** and **2** (see Fig. 4 and S23†) albeit an obvious difference in magnitude for their energy barriers is visible. Consistently, zero field and

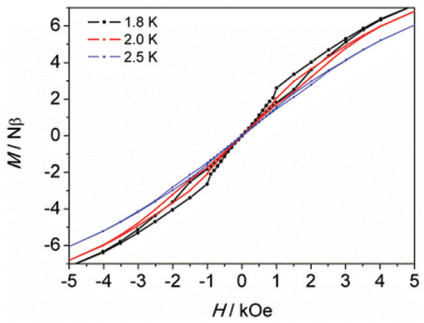

Fig. 4 Plots of magnetizations (*M*) *versus* dc field for **1**.

field-cooled magnetic susceptibility data collected for **1** and **2** show a divergence at around 2.2 K (Fig. S6†).

Recently, an organometallic dinuclear system $[(Cp^*_2Ln)_2(\mu\text{-bpym}^{\bullet})]^+$ was reported in which lanthanide ions were bridged by the radical $BPYM^{\bullet-}$ anion.[14] The antiferromagnetic coupling constant about −10 cm^{-1} favoured the Dy2 system to display a 87.8 cm^{-1} energy barrier and magnetic hysteresis up to 6.5 K with the average sweep rate of 0.002 T s^{-1}. In our case, the neutral bridging BPYM was proposed to transmit a very weak antiferromagnetic coupling with Dy(III) ions, according to recent research,[15] whereas the significant magnetic relaxation behaviour with higher energy barriers was still observed. The magnetic dilution experiment reveals that the relaxation mainly comes from individual Dy(III) ions for the suitable ligand field and local symmetry. The weak magnetic couplings in these two systems were not dominant factors for relaxation.

Conclusions

In conclusion, air-stable dinuclear SMMs were efficiently constructed by two isolated β-diketonate Dy(III) segments through a neutral BPYM bridging ligand. The existence of different solvents in the molecule lattice leads to distinct crystal structures with one and two kinds of coordination environment around Dy(III) ions, respectively, that results in distinct dynamic magnetic relaxations. These systems show relative high energy barriers for the reversal of magnetization and magnetic hysteresis temperature, which reveals that the particular local coordination symmetry may play a crucial role in dynamic relaxations, even under a weak magnetic exchange interaction between the spin carriers.

Acknowledgements

This work was supported by the NSFC (21290171, 21321001, 21372014, 21441007, 21102039 and 21572048), BJSFC (2122023) and the National Basic Research Program of China (2013CB933401, 2010CB934601), the BNLMS (20140108), and the Educational Commission of Heilongjiang Province (1254G045, 12541639).

Notes and references

1 N. Ishikawa, M. Sugita, T. Ishikawa, S. Koshihara and Y. Kaizu, *J. Am. Chem. Soc.*, 2003, **125**, 8694–8695.
2 R. Sessoli, D. Gatteschi, A. Caneschi and M. A. Novak, *Nature*, 1993, **365**, 141–143.
3 D. Gatteschi, R. Sessoli and J. Villain, *Molecular Nanomagnets*, Oxford University Press, Oxford, 2006.
4 J. van Slageren, *Top. Curr. Chem.*, 2012, **321**, 199–234.
5 D. Gatteschi and R. Sessoli, *Angew. Chem., Int. Ed.*, 2003, **42**, 268–297.
6 L. Bogani and W. Wernsdorfer, *Nat. Mater.*, 2008, **7**, 179–186.
7 R. Vincent, S. Klyatskaya, M. Ruben, W. Wernsdorfer and F. Balestro, *Nature*, 2012, **488**, 357–360.
8 C. R. Ganivet, B. Ballesteros, G. de la Torre, J. M. Clemente-Juan, E. Coronado and T. Torres, *Chem. – Eur. J.*, 2013, **19**, 1457–1465.
9 J. D. Rinehart, M. Fang, W. J. Evans and J. R. Long, *Nat. Chem.*, 2011, 538–542.
10 (*a*) J. D. Rinehart, M. Fang, W. J. Evans and J. R. Long, *J. Am. Chem. Soc.*, 2011, **133**, 14236–14239; (*b*) F. Habib and M. Murugesu, *Chem. Soc. Rev.*, 2013, **42**, 3278–3288; (*c*) E. M. Pineda, N. F. Chilton, R. Marx, M. Dörfel, D. O. Sells, P. Neugebauer, S. D. Jiang, D. Collison, J. van Slageren, E. J. L. McInnes and R. E. P. Winpenny, *Nat. Commun.*, 2014, **5**, 5243; (*d*) Y. C. Chen, J. L. Liu, L. Ungur, J. Liu, Q. W. Li, L. F. Wang, Z. P. Ni, L. F. Chibotaru, X. M. Chen and M. L. Tong, *J. Am. Chem. Soc.*, 2016, **138**, 2829–2837.
11 (*a*) T. Fukuda, N. Shigeyoshi, T. Yamamura and N. Ishikawa, *Inorg. Chem.*, 2014, **53**, 9080–9086; (*b*) E. Lucaccini, L. Sorace, M. Perfetti, J. P. Costes and R. Sessoli, *Chem. Commun.*, 2014, **50**, 1648–1651; (*c*) K. S. Pedersen, L. Ungur, M. Sigrist, A. Sundt, M. Schau-Magnussen, V. Vieru, H. Mutka, S. Rols, H. Weihe, O. Waldmann, L. F. Chibotaru, J. Bendix and J. Dreiser, *Chem. Sci.*, 2014, **5**, 1650–1660; (*d*) J. L. Liu, K. Yuan, J. D. Leng, L. Ungur, W. Wernsdorfer, F. S. Guo, L. F. Chibotaru and M. L. Tong, *Inorg. Chem.*, 2012, **51**, 8538–8544.
12 W. B. Sun, B. Yan, Y. Q. Zhang, B. W. Wang, Z. M. Wang, J. H. Jia and S. Gao, *Inorg. Chem. Front.*, 2014, **1**, 503–509.
13 R. Ilmi and K. Iftikhar, *Polyhedron*, 2015, **102**, 16–26.
14 (*a*) S. Demir, J. M. Zadrozny, M. Nippe and J. R. Long, *J. Am. Chem. Soc.*, 2012, **134**, 18546–18549; (*b*) W. Yu, F. Schramm, E. M. Pineda, Y. Lan, O. Fuhr, J. Chen, H. Isshiki, W. Wernsdorfer, W. Wulfhekel and M. Ruben, *Beilstein J. Nanotechnol.*, 2016, **7**, 126–137.
15 (*a*) G. Zucchi and X. F. Le Goff, *Polyhedron*, 2013, **52**, 1262–1267; (*b*) M. H. Baker, J. D. Dorweiler, A. N. Ley, R. D. Pike and S. M. Berry, *Polyhedron*, 2009, **28**, 188–194; (*c*) J. Vallejo, J. Cano, I. Castro, M. Julve, F. Lloret, O. Fabelo, L. Cañadillas-Delgado and E. Pardo, *Chem. Commun.*, 2012, **48**, 7726–7728.

16 M. Llunell, D. Casanova, J. Cirera, P. Alemany and S. Alvarez, *SHAPE, v2.1*, University of Barcelona and The Hebrew University of Jerusalem, Barcelona and Jerusalem, 2013.
17 S. Titos-Padilla, J. Ruiz, J. M. Herrera, E. K. Brechin, W. Wersndorfer, F. Lloret and E. Colacio, *Inorg. Chem.*, 2013, **52**, 9620–9626.
18 E. Colacio, J. Ruiz, E. Ruiz, E. Cremades, J. Krzystek, S. Carretta, J. Cano, T. Guidi, W. Wernsdorfer and E. K. Brechin, *Angew. Chem., Int. Ed.*, 2013, **52**, 9130–9134.
19 A. Abragam and B. Bleaney, *Electron Paramagnetic Resonance of Transition Ions*, Clarendon Press, Oxford, U.K., 1970.
20 K. N. Shirivastava, *Phys. Status Solidi B*, 1983, **117**, 437–458.
21 Y. Bi, Y. N. Guo, L. Zhao, Y. Guo, S. Y. Lin, S. D. Jiang, J. K. Tang, B. W. Wang and S. Gao, *Chem. – Eur. J.*, 2011, **17**, 12476–12481.
22 G. J. Chen, Y. N. Guo, J. L. Tian, J. K. Tang, W. Gu, X. Liu, S. P. Yan, P. Cheng and D. Z. Liao, *Chem. – Eur. J.*, 2012, **18**, 2484–2487.